

## Characteristics of a cucurbit[5]uril adsorption layer on the electrode/solution interface

Elena V. Stenina and Liana N. Sviridova\*

Department of Chemistry, M. V. Lomonosov Moscow State University, 119991 Moscow, Russian Federation.

Fax: +7 495 939 0171; e-mail: slianan@mail.ru, estenina@yandex.ru

DOI: 10.1016/j.mencom.2015.01.022

The behavior of cucurbit[5]uril at the electrode/solution interface was quantified in wide ranges of electrode potentials and adsorbate concentrations.

Cucurbit[5]uril ( $C_6H_6N_4O_2$ )<sub>5</sub> is the smallest member of the homological series of cucurbit[*n*]urils, a group of cyclic, pumpkin-shaped molecules composed of *n* glycoluril units bridged by methylene bridges (Figure 1). The bottom and top planes of these kegs represent cavity portals formed by carbonyl groups. This unique feature allows cucurbiturils to encapsulate organic molecules or ions in their hydrophobic inner cavity and simultaneously bind metal cations due to their interaction with carbonyl groups at the portals. This property and the structural rigidity of cucurbituril molecules make them attractive as building blocks for synthesizing supramolecular compounds and developing new hybrid organo-inorganic materials on their basis. Thus, cucurbiturils are important synthons in supramolecular chemistry. Both these compounds and their host–guest complexes are of considerable current interest.<sup>1</sup> The adsorption of compounds from this series on gold and semiconductor (TiO<sub>2</sub>) surfaces has been studied,<sup>2,3</sup> which is very important for the development of sensors and solar cells.

The properties of adsorbed layers of cucurbit[*n*]urils on the electrode/solution interface have not been studied so far. The aim of this work was to study the adsorption of cucurbit[5]uril (CB5) on the Hg-electrode/0.1 M Na<sub>2</sub>SO<sub>4</sub> solution interface. The crystals of this cyclic pentamer were synthesized and structurally characterized.<sup>4</sup> The outer diameter and the height of the CB5 molecule are 1.31 and 0.91 nm, respectively. The inner cavity diameter is 0.44 nm and the cavity volume is 0.082 nm<sup>3</sup>. The solubility of this compound in water substantially increases with the addition of ammonium, alkali and alkali-earth metal salts. With the Na<sup>+</sup> cation, CB5 forms a 1:1 complex with the stability constant  $\lg K_s = 1.85$ .<sup>5,†</sup>

The differential capacity vs. potential (*C* vs. *E*) curves for a mercury electrode were measured in 0.1 M Na<sub>2</sub>SO<sub>4</sub> solutions containing 10<sup>-3</sup>–5×10<sup>-7</sup> mol dm<sup>-3</sup> CB5 (Figure 1). In these solutions, *C* is lower than that of the background solution over an

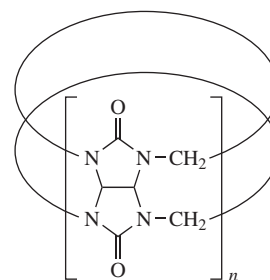


Figure 1 Molecular structure of CB[*n*] molecules.

unusually wide potential range (~2 V), *i.e.*, the adsorption of this compound occurs. For physically adsorbed organic surfactant layers, this region is ~1 V, for instance, for two-dimensional condensed layers formed by molecules with cage-like structures (adamantanol and camphor).<sup>6</sup> The adsorption of CB5 proceeds at both positive and negative charges of the electrode surface [the electrode potential of zero charge (PZC) in the background solution  $\varphi_{zcp}$  is -0.44 V (vs. SCE)]. The considerable extension of the CB5 adsorption range to negative potentials, as compared with the above surfactants, suggests that the adsorbed species is positively charged at these potentials. At the limiting negative potentials (~ -1.9 V), a sharp increase in the capacitance was observed in all of the test systems, which was associated with the electrochemical reduction of Na<sup>+</sup> rather than the desorption of CB5 from the electrode surface. At the same time, the positive charge of a species should prevent its adsorption at positive surface charges due to electrostatic repulsion. The fact that the adsorption of CB5 was also experimentally observed at positive charges can be explained assuming that the charge of the adsorbed species is different in the potential ranges corresponding to negative and positive electrode charges.

A structural arrangement is also indicated by *C* variations in the CB5 adsorption regions with variations of the potential. The lowest *C* values corresponding to a relatively thick adsorption layer pertain to the region of negative potentials.<sup>‡</sup> Note that a transition between these two regions in the *C* vs. *E* curves corresponding to different *C* values takes place precisely at the PZC observed in the background solution. This experimental observation confirms the assumption that the charge of the adsorbed species changes as we pass through this point during potential scanning. Henceforth, we designate the adsorption

‡ A certain increase in the capacitance in the middle of this region observed for relatively low CB5 concentrations points to slight changes in the adsorbate structure.

† The studies were carried out on a hanging mercury drop electrode by measuring the differential capacitance *C* as a function of potential *E* by means of an Autolab potentiostat–galvanostat at a frequency *f* = 370 Hz and an ac voltage amplitude of 1 mV. The working electrode potential was varied in steps of 25 mV. The *C* vs. *E* curves were recorded with time (*t* = 10 s) of the electrode exposure at each potential. A mercury drop with a surface area of 0.015 cm<sup>2</sup> (determined by weight) was formed at the end of a conical capillary with an inner diameters of 80 μm by a special tool included in a PA-3 polarographic analyzer (Czech Republic). The electrode potentials were measured with respect to SCE. Cucurbit[5]uril (Aldrich) was used without additional purification; Na<sub>2</sub>SO<sub>4</sub> was twice crystallized; and water was cleaned on a Millipor unit. Solutions were deaerated with high purity argon.

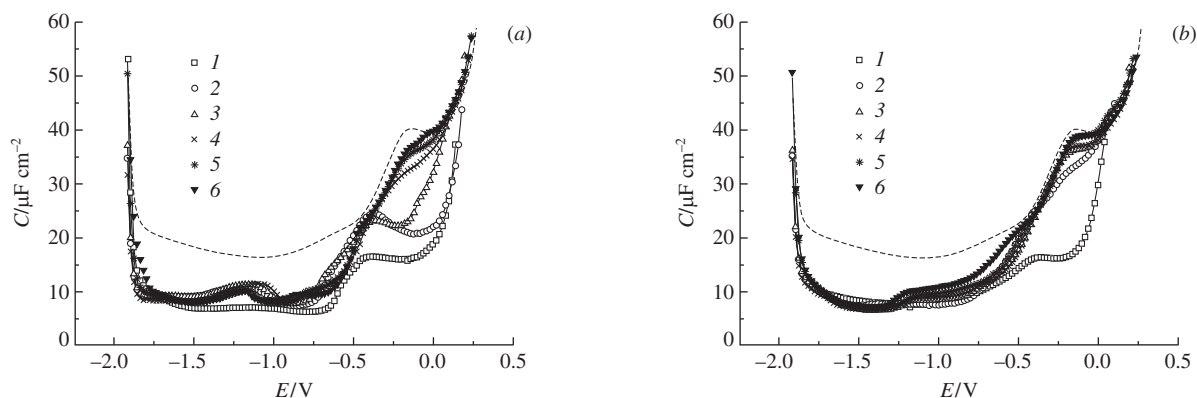


**Figure 2** Experimental  $C$  vs.  $E$  curves of a Hg electrode in 0.1 M  $\text{Na}_2\text{SO}_4$  in the presence of CB5 in concentrations (1)  $10^{-3}$ , (2)  $2.5 \times 10^{-4}$ , (3)  $10^{-4}$ , (4)  $5 \times 10^{-5}$ , (5)  $10^{-5}$  and (6)  $2 \times 10^{-6}$  mol  $\text{dm}^{-3}$ , obtained by potential scanning (a) from negative to positive and (b) from positive to negative  $E$  values. Dashed line is the  $C$  vs.  $E$  curve in 0.1 M  $\text{Na}_2\text{SO}_4$ .

regions at the negative and positive electrode surface charges as regions I and II, respectively.

A comparison between Figures 2(a) and 2(b) leads us to the conclusion that  $C$  at positive electrode charges substantially depends on the potential scan direction. This hysteresis effect is the most pronounced for relatively low CB5 concentrations. In the region of negative surface charges, a noticeable hysteresis was observed only for CB5 concentrations below  $10^{-6}$  mol  $\text{dm}^{-3}$  at the boundaries of this region, while limiting surface coverages were reached in its central part regardless of the CB5 concentration.

The above data testify to a substantial difference in the properties of CB5 adsorbed layers formed at the opposite charges of the electrode surface. Therefore, the parameters characterizing these adsorbates were calculated using only a relevant part of the overall impedance data array corresponding to the equilibrium conditions. For the negatively charged electrode surface, a series of  $C$  vs.  $E$  curves for the highest concentrations ( $10^{-3}$ – $2.5 \times 10^{-4}$  mol  $\text{dm}^{-3}$  CB5) in a potential range from  $-1.1$  to  $-0.5$  V measured in the positively directed potential scan was selected for calculation. In the region of positive electrode surface charges, only the  $C$  vs.  $E$  curve for  $10^{-3}$  mol  $\text{dm}^{-3}$  CB5 measured from  $E = +0.1$  V in the negatively directed potential scan was selected for calculation.

The experimental data were processed by a regression analysis technique<sup>7</sup> using the maximum adsorption potential  $\varphi_m$  in the rational potential scale, the logarithm of the constant of adsorption equilibrium at the maximum adsorption potential  $\ln B_m$ , the intermolecular interaction parameter in the adsorption layer  $a_m$  for  $\varphi = \varphi_m$ , the capacitance  $C_m$  at the limiting surface coverage with organic molecules ( $\theta = 1$ ) and  $\varphi = \varphi_m$ , and the parameter  $A = RT\Gamma_m$ , where  $\Gamma_m$  is the limiting surface concentration of the organic substance for  $\theta = 1$  and  $R$  and  $T$  have their usual meanings. The parameter  $\varphi_N$  characterizing zero charge potential variations upon a transition from  $\theta = 0$  to  $\theta = 1$  was found based on the  $\varphi_m$  value.<sup>7</sup>

Table 1 summarizes the parameters of a CB5 adsorption layer found for the two potential regions. A comparison of data in Figure 3 for region II shows that the experimental  $C$  values for the lowest CB5 concentrations considerably exceed the calculated values. As noted above, under conditions of this experiment, the equilibrium  $C$  values were not reached.

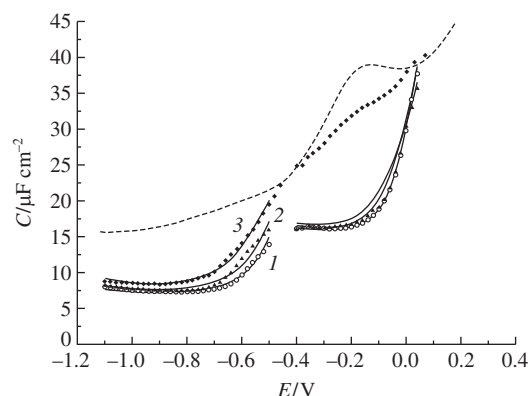


**Figure 3**  $C$  vs.  $E$  curves of a Hg electrode in 0.1 M  $\text{Na}_2\text{SO}_4$  in the presence of CB5 in concentrations (1)  $10^{-3}$ , (2)  $5 \times 10^{-4}$  and (3)  $2.5 \times 10^{-4}$  mol  $\text{dm}^{-3}$ . Points refer to experimental data and lines were calculated with adsorption parameters obtained for the potential ranges:  $-1.1$  to  $-0.6$  V and  $+0.1$  to  $-0.4$  V. Dashed line is the  $C$  vs.  $E$  curve in 0.1 M  $\text{Na}_2\text{SO}_4$ .

Regions I and II in the experimental  $C$  vs.  $E$  curves correspond to adsorption layers with different properties because the corresponding adsorption parameters are substantially different in these regions. The largest deviation (by a factor of more than 2) is typical of the maximum adsorption values of these layers. In region II,  $\Gamma_m$  corresponds to the almost complete surface coverage, amounting to 88% of the theoretically maximum value of  $1.23 \times 10^{-10}$  mol  $\text{cm}^{-2}$ , which correlates with the area occupied by a single CB5 molecule oriented with the oxygen groups of its portal to the electrode surface. This orientation was experimentally observed for the adsorption of CB6 and CB7 molecules on an uncharged gold surface.<sup>2</sup> In this case, the almost complete surface coverage can be reached only for the adsorption of neutral ligands on the electrode surface. The complete surface coverage by cationic complexes corresponds to an adsorbate layer with the overall charge above  $10 \mu\text{C cm}^{-2}$ . The presence of such a layer on the electrode surface with a charge of the same sign is physically unreal. Therefore, the experimentally observed fact that the formation of an adsorbed layer in region II is slow is quite understandable. Indeed, the concentration of positively charged complex species near the positively charged electrode

**Table 1** Adsorption parameters of the complex formed in the solutions of cucurbit[5]uril +  $\text{Na}_2\text{SO}_4$ .

Electrode potential range/V	$\varphi_m$ /V	$\ln B_m$	$A/\mu\text{J cm}^{-2}$	$\Gamma_m/10^{10}$ mol $\text{cm}^{-2}$	$-\Delta G_m/\text{kJ mol}^{-1}$	$a_m$	$C_m/\mu\text{F cm}^{-2}$	$\varphi_N$ /V	$\Delta$ (%)
+0.1 to -0.4	0.16	14.4	0.27	1.1	45.6	-1.8	15.8	-0.15	0.7
-1.1 to -0.6	-0.47	8.4	0.58	2.3	30.9	1.0	6.9	0.92	3.2

surface is lower than at negative charges; moreover, the formation of an adsorption layer from neutral species should be preceded by the stage of dissociation of the cationic complex to form neutral CB5 molecules.

The much faster formation of an adsorbate layer at the negatively charged electrode surface can be explained by the fact that the adsorbed species are positively charged complexes that occur in solution. In region I (excluding its boundary parts), the  $C$  values are independent of the electrode exposure time at a given potential and also of the CB5 concentration. It follows from Table 1 that, in the latter region, the  $F_m$  value is more than two times higher than that in region II, and the limiting capacitance is less than a half of the corresponding value in the region of a positively charged electrode surface. This can be explained by the formation of an adsorption bilayer in region I due to the ion–dipole interactions of the  $\text{Na}^+$  cations with the oxygen portals of two CB5 cavitands. The formation of such a bilayer was reported<sup>2</sup> for a CB6 adsorption layer on gold in the presence of  $\text{Na}^+$ . In the absence of these cations the formation of a monolayer was observed.

In region I,  $\varphi_N$  has a large positive value, which points to a severe positive shift of  $\varphi_{zcp}$ , *i.e.*, to the adsorption of the organic cation. The opposite-sign shift of  $\varphi_{zcp}$  in region II corresponds to the adsorption of CB5 species oriented with the carbonyl groups at their portal to the electrode surface. The negative value of  $a_m$  in region II reflects the repulsive interaction of adsorbed species due to the presence of portals edged with carbonyl groups. In region I, the repulsive interaction gives a way to attraction ( $a_m$  becomes positive) because the effect of carbonyl groups weakens owing to the ion–dipole interaction with  $\text{Na}^+$  cations. The dielectric permittivity of CB5 adsorption layers was assessed using plane-capacitor equations. The found average permittivity value is  $\sim 15$ , which is high because of a large number of polar carbonyl groups (10) in the CB5 molecule. Analogous estimates afforded a dielectric permittivity of 3 for the adsorption layer of adamantanol molecules (one oxygen atom per molecule) or 7 for cryptand[2.2.2] (six oxygen atoms).

The complicated adsorption behavior of CB5 in the presence of  $\text{Na}^+$  cations is associated with the fact that this cavitand can

form complexes with cations by binding them through the oxygen groups of external portals rather than through their inclusion into the internal cavity. Moreover, the effect of the environment on the bound cations is preserved to a considerable extent. The dependence of the adsorption layer properties on the electrode surface charge was also observed in diprotonated cryptand[2.2.2] in which one of protons was localized outside the internal cavity of this macrobicycle.<sup>8</sup> However, the complex behavior described above is untypical of inclusion cryptate complexes of inorganic cations.<sup>9,10</sup> Probably, this can be explained by the strong screening of the positive charge of a species after its inclusion into the internal cavity of an organic ligand, which considerably weakens its interaction with the environment.<sup>11</sup>

This study was supported by the Russian Foundation for Basic Research (grant no. 14-03-00706).

## References

- 1 E. Masson, X. Ling, R. Joseph, L. Kyeremeh-Mensah and X. Lu, *RSC Adv.*, 2012, **2**, 1213.
- 2 E. Blanco, C. Quintana, L. Hernandez and P. Hernandez, *Electroanalysis*, 2013, **25**, 263.
- 3 M. Freitag and E. Gallopini, *Langmuir*, 2010, **26**, 8262.
- 4 A. Flinn, G. C. Hough, J. F. Stoddart and D. J. Williams, *Angew. Chem., Int. Ed. Engl.*, 1992, **31**, 1475.
- 5 H.-J. Buschmann, E. Cleve, K. Jansen, A. Wego and E. Schollmeyer, *J. Incl. Phenom.*, 2001, **40**, 117.
- 6 E. V. Stenina and B. B. Damaskin, *J. Electroanal. Chem.*, 1993, **349**, 31.
- 7 B. B. Damaskin, V. A. Safonov and O. A. Baturina, *Russ. J. Electrochem.*, 1997, **33**, 105 (*Elektrokhimiya*, 1997, **33**, 117).
- 8 E. V. Stenina and L. N. Sviridova, *Russ. J. Electrochem.*, 2012, **48**, 150 (*Elektrokhimiya*, 2012, **48**, 165).
- 9 E. V. Stenina and L. N. Sviridova, *Russ. J. Electrochem.*, 2005, **41**, 414 (*Elektrokhimiya*, 2005, **41**, 475).
- 10 E. V. Stenina and L. N. Sviridova, *Mendeleev Commun.*, 2013, **23**, 282.
- 11 J.-M. Lehn, *Pure Appl. Chem.*, 1980, **52**, 2303.

Received: 14th April 2014; Com. 14/4351